HYPERSPECTRAL LINEAR UNMIXING: QUANTITATIVE EVALUATION OF NOVEL TARGET DESIGN AND EDGE UNMIXING TECHNIQUE

Daniel S. Goldberg, John P. Kerekes, Kelly A. Canham

Chester F. Carlson Center for Imaging Science
Rochester Institute of Technology, Rochester, NY

ABSTRACT

Remotely sensed hyperspectral images (HSI) have the potential to provide large amounts of information about a scene. HSI, in this context, are images of the Earth collected with a spatial resolution of 1m to 30m in dozens to hundreds of contiguous narrow spectral bands over different wavelengths so that each pixel is a vector of data. Spectral unmixing is one application which can utilize the large amount of information in HSI. Unmixing is a process used to retrieve a material's spectral profile and its fractional abundance in each pixel since a single pixel contains a mixture of material spectra. Unmixing was used with images collected during an airborne hyperspectral collect at the Rochester Institute of Technology in 2010 with 1m resolution and a 390nm to 2450nm spectral range. The goal of our experiment was to quantitatively evaluate unmixing results by introducing a novel unmixing target. In addition, a single-band, edge unmixing technique is introduced with preliminary experimentation which showed results with mean unmixing fraction error of less than 10%. The results of the methods presented above helped in the design of future collection experiments.

Index Terms— hyperspectral, spectral unmixing, validation, edge unmixing

1. INTRODUCTION

Remotely sensed hyperspectral imagery (HSI) is often used to analyze large scenes on the Earth. For most Earth observation, HSI are defined as images collected with spatial resolution of around 1m to 30m ground pixels with hundreds of contiguous narrow spectral bands.

HSI is used for a wide variety of applications [1]. The particular application considered here is material mapping which can take advantage of the high spectral resolution. It is often the case that a scene will have a variety of materials in it. "Spectral unmixing" is a way to utilize the high spectral information in HSI to map surface materials at sub-pixel levels. The simplest and most common model for spectral unmixing is the linear mixture model (LMM). However, there has not been much quantitative evaluation of unmixing techniques using real world data due to the challenge of accurately knowing the material fractions present.

This paper provides the background and motivation of the pixel unmixing application in section 2. We discuss the linear spectral unmixing method, novel target, and present some results in section 3. Next, a new technique for validating retrieved material fractions is proposed which focuses on two distinct, adjacent materials along an edge using only a single spectral band in section 4. Finally, a conclusion is made from the results of the two experiments and future work is discussed in section 5.

2. BACKGROUND AND MOTIVATION

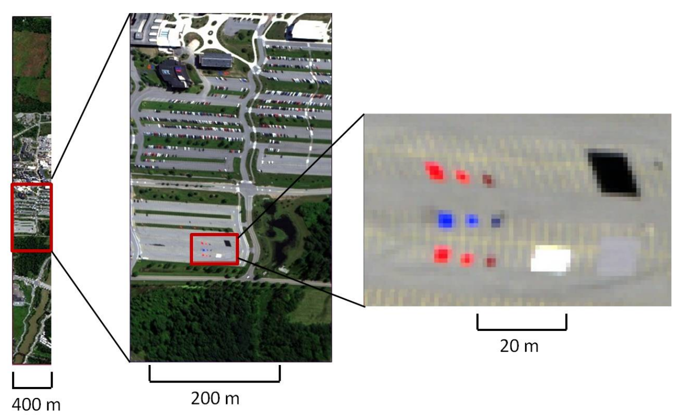

Fig. 1. The whole flight line (left) and the subset used (right).

Spectral unmixing is a widely used application of HSI, though the quantitative evaluation of unmixing results has been challenging. Unmixing is often done on a large scene but precise ground-truth measurements of material fractional abundances per pixel are usually unknown. A novel target has been proposed which hopes to give a method of testing the unmixing process by introducing a target with a known fractional abundance. The target was deployed in a data collect to investigate the validity of using such a target in a real-world scene.

In 2010 a large scale airborne and ground experiment data collection was undertaken at Rochester Institute of Technology, courtesy of SpecTIR [2]. It came to be known as SpecTIR Hyperspectral Airborne Rochester Experiment (SHARE 2010). SpecTIR flew their ProSpecTIR-VS2 instrument at various elevations to achieve various spatial resolutions. The unmixing target (described further in section 3.2) was designed for the 1m spatial resolution flight lines. The instrument had a spectral coverage of 360 bands from 400nm to 2400nm. There were four flight lines over various locations at 1m resolution. The flight line that was used in our experiment is shown in Fig. 1. This flight line was repeated, with one pass at 3:19 PM and one pass at 3:40 PM.

3. LINEAR SPECTRAL UNMIXING

Detailed analysis of materials within a scene can be accomplished when sufficient spectral information is known. Spectral unmixing is a technique by which a single pixel is broken down into constituent vectors (called endmembers and representing pure materials) and the amount of each vector (called fractional abundance) [3]. A precondition of this technique is that all endmembers' vectors are known. Unmixing is needed because in most cases, areas in a scene are not pure materials but mixtures of materials. Also, when dealing with airborne imagery, relatively low spatial resolution is common which causes mixed pixels [3].

3.1. The Method of Linear Spectral Unmixing

The linear mixing model (LMM) assumes that each mixture is a linear combination of the endmember spectra. This paper only focuses on the LMM for analysis of the novel unmixing target. Since the method for unmixing is out of the scope of the experiment, other non-linear techniques were not employed. Equation 1 shows the model for a single received pixel, $\mathbf{x}$, with N spectral bands and M endmembers. In this situation, $\mathbf{x}$ is an $N \times 1$ vector, $\mathbf{A}$ is an $N \times M$ matrix where a single column is an $N \times 1$ endmember spectrum, and $\mathbf{f}$ is a $1 \times M$ vector of the fractional abundance of each endmember. In addition, $\mathbf{w}$ is an additive observation, zero-mean, noise vector which also has dimensions of $N \times 1$.

$$\begin{bmatrix} \mathbf{x}_1 \\ \vdots \\ \mathbf{x}_N \end{bmatrix} = \begin{bmatrix} \mathbf{a}_{11} & \cdots & \mathbf{a}_{1M} \\ \vdots & \ddots & \vdots \\ \mathbf{a}_{N1} & \cdots & \mathbf{a}_{NM} \end{bmatrix} \begin{bmatrix} \mathbf{f}_1 & \cdots & \mathbf{f}_M \end{bmatrix} + \begin{bmatrix} \mathbf{w}_1 \\ \vdots \\ \mathbf{w}_N \end{bmatrix} \tag{1}$$

$$\left(\mathbf{A}^T * \mathbf{A}\right)^{-1} \mathbf{A}^T \mathbf{x} = \mathbf{f} \tag{2}$$

Equation 2 shows the solution of equation 1 when solving for the abundance fraction for each material. This simple matrix operation does not necessarily constrain the abundance fractions for a pixel to sum to unity. Also, individual fractions could be less than zero [3]. Non-linear constraints to limit these unrealistic outputs were not imposed. Constrained unmixing provided less consistent results possibly due to imperfections in endmember selection in the scene.

When applying the LMM to a subset of the flight line shown in Fig. 1, eight pixels were manually selected as endmembers. After subsetting the image spatially, spectral subsets were tested. The spectral range of SpecTIR's instrument is a combination of a visible and near infrared (VNIR) instrument and a short wave infrared (SWIR) instrument. In addition to spectral range, multiple combinations of various processing steps were tested. We will only present and discuss cases which significantly impacted the results.

3.2. Novel Target Design

Due to the limited accurate ground truth for pixel fractional abundances in natural scenes, a target design has been introduced to allow for analysis of spectral unmixing (target shown in Fig. 2). The key to the target is that the area in the image will produce at least one pixel with a known, specific fractional abundance. In the case of the target designed for SHARE 2010 (section 2) fabric squares (of a single material) on a black background were laid out so that a 25% fractional abundance of fabric is expected. The design in Fig. 2 shows that four small fabric squares will fall inside a pixel of size 1m^2 (Fig. 2). No matter how precisely aligned with the target, 25% of a pixel will be filled by the fabric.

During SHARE 2010, three sets of three targets with three different materials were deployed as seen in Fig. 1. Each row of targets seen in the figure includes a large 3m $\times$ 3m pure material, a small 2m$\times$2m pure material, and then the 2m$\times$2m unmixing target.

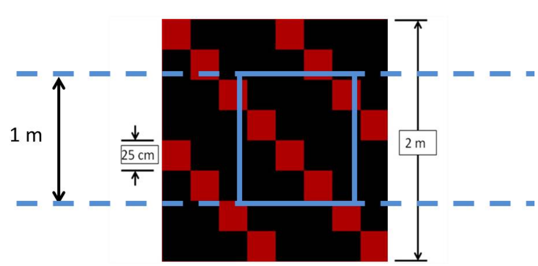

Fig. 2. Novel target design used in SHARE 2010 with overlay of example sensor pixel.

3.3. Results of Novel Target Design

Results of the three unmixing targets made from various materials are analyzed here. The goal, stated in section 3.2, is to validate the expected 25% fractional abundance for each unmixing target. The retrieved fractional abundances are shown in Fig. 3. The values were were lower than expected. The findings will be discussed further in section 5.

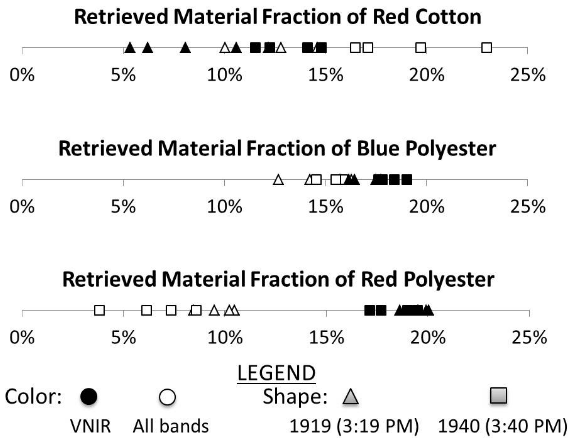

Fig. 3. Results of the unmixing process for each material, at both times, and using two separate spectral subsets.

4. EDGE UNMIXING

Edge unmixing is a method to unmix two adjacent contrasting materials across an edge. In its current implementation it uses only a single spectral band, though, it can be expanded to work on individual bands of HSI. For one band, the algorithm models the edge, and computes the subpixel distance from a center to the edge location. For an edge, the intensity at a pixel depends on how much of the edge covers that pixel.

To estimate the edge location, this algorithm requires that an edge falls across multiple lines and that the spatial resolution be high enough that the edge makes a noticeable difference in the intensity for that pixel. This method was evaluated using simulated intensity images generated by downsampling a high resolution image of a rotated square, applying a low resolution point spread function, and adding zero mean noise.

4.1. Edge Unmixing Algorithm

The edge must be estimated with subpixel accuracy. To do this, first the edge is determined to be primarily horizontal or vertical. Next, the directional derivative is taken along multiple columns (or rows) perpendicular to the edge to find the location of maximum change along the pixels. Finding this maximum will reveal where the edge falls in a pixel and, in turn, find where the edge falls in a set of pixels. An example plot of the line spread functions (derivatives across the edge) is shown in Fig. 4. To estimate the location of the maximum, a Gaussian fit was applied and the data were oversampled. After finding the peak of each Gaussian, a linear regression was fit to the peak and RANSAC [4] was used to remove outliers. Using the remaining data, a linear least squares regression was fit to the locations in order to find the location of the edge with subpixel accuracy across the pixels. The calculated edge is shown plotted on top of a simulated target in Fig. 5.

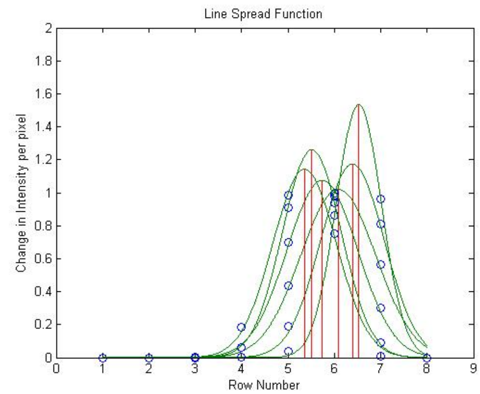

Fig. 4. Plots of oversampled line spread functions with peaks and original points.

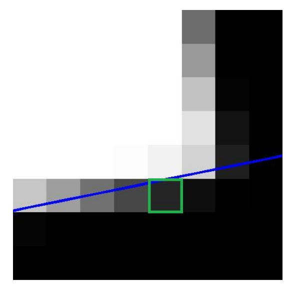

Fig. 5. Simulation showing where the edge enmixing algorithm found the edge. Outlined pixel shows a location where corners cause inaccurate unmixing results.

After the edge is found, the distance is found from the peak pixel location to the line location in order to estimate how much of that material is in a pixel. The distance from the original peak pixel to the interpolated line is the unmixing amount. It is important to note that the line must be shifted by half a pixel so that the line is located at the front of each pixel, not in the middle.

The pixel outlined in Fig 5 shows a corner pixel which the calculated edge passes through. Confusion occurs at corners where the transition from a horizontal edge to vertical edge occurs. This causes large RMS errors since the estimated line continues past the corner.

4.2. Results of Edge Unmixing

A simulated edge with varying spatial resolution, angle relative to image orientation, and noise was used to test the algorithm. Section 5 discusses how this unmixing approach will be tested in the future.

Fig. 6 shows the RMS error of the fractional abundance plotted against the target orientation in degrees. It shows how the algorithm performs as the edge is rotated from 0 degrees

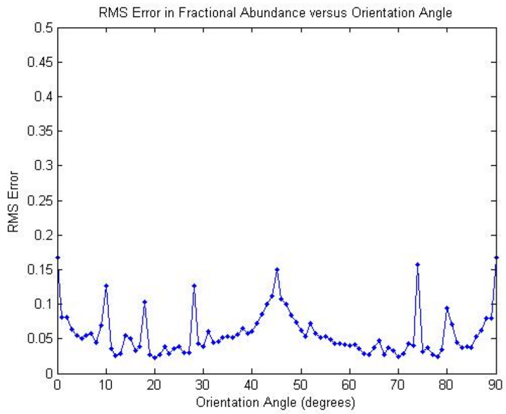

Fig. 6. Results of the edge unmixing process for an edge of white on a black background.

to 90 degrees relative to the horizontal. A possible cause of the noisy higher frequency peaks around 10 degrees and 75 degrees is misclassification of corner pixels leading to drastic miscalculations of fractional abundance. The effect of corners will be looked into in future studies.

Edge unmixing performed well overall on the simulation images showing a mean RMS error of 6% fractional abundance. Orientation angles at the extremes showed worse performance than those between. This is due to large changes in the line spread functions at more extreme angles. The large differences in the line spread functions causes poor interpolation of an edge through the pixels.

In addition to orientation, spatial resolution was tested. To test how the spatial resolution of an edge affected the results, an edge with an orientation of 15 degrees was generated at various resolutions. Fig. 7 shows the unmixing fractional abundance versus the image size in pixels (the resolution is lower for smaller image sizes). This figure shows that we can expect the best results from an edge length of at least 7 pixels.

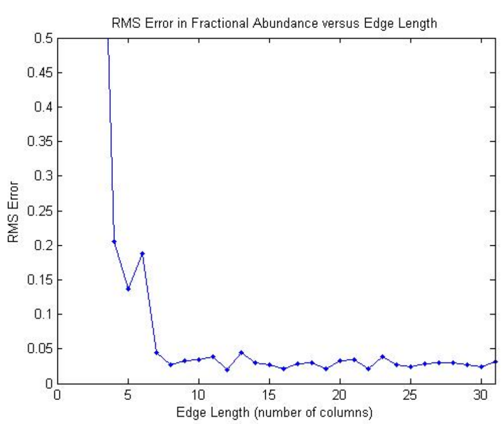

Fig. 7. Plot showing the calculated unmixing fraction versus the number of columns (or rows) of pixels an edge runs along.

5. CONCLUSIONS AND FUTURE WORK

In conclusion, two new approaches to validating spectral unmixing were introduced. In the case of the unmixing target, the results showed that actual unmixing fractional abundances tended to under-estimate the amount of the true fractional abundances. The overall pixel fraction was about 5% to 10% lower than expected. This is most likely due to scattering of the energy from the small target which became diminished by the scatter from the asphalt surrounding it. Also, the $1\text{m} \times 1\text{m}$ box representing the point spread function of the system is an idealized view. In reality, the pixel is integrating over an approximate Gaussian with a full width half max of 1m. The target design could be improved by increasing its size to reduce the possibility of adjacency effects from outside materials.

The preliminary, proof-of-concept edge unmixing results proved that this method could be used in the right situation. Further testing needs to be done with real-world data using a variety of spectral bands. Also, the additional complication of geometric registration of images arises since airborne systems have constantly changing three dimensional rotations (eg. the yaw, pitch, and roll of an aircraft). Though its current implementation works with line edges, the algorithm could be expanded to work with curvilinear edges if the subpixel location of the edge can be modelled.

The results of both experiments provided information necessary to redesign experiments for a new data collect. From the knowledge gained in the work described here, targets for both applications were designed for a new data collection taken in September of 2012.

6. ACKNOWLEDGEMENTS

RIT colleagues Jared Herweg and Paul Romanczyk are acknowledged for their helpful discussions.

7. REFERENCES

[1] J. R. Schott, *Remote Sensing: The Image Chain Approach*, Oxford University Press, USA, 2007.

[2] J. A. Herweg, J. P. Kerekes, O. Weatherbee, D. Messinger, J. van Aardt, E. J. Ientilucci, Z. Ninkov, J. Faulring, Nina Raqueo, and J. Meola, “Spectir hyperspectral airborne rochester experiment data collection campaign,” in *Proc. SPIE 8390*, May 2012.

[3] N. Keshava and J. F. Mustard, “Spectral unmixing,” *Signal Processing Magazine, IEEE*, vol. 19, no. 1, pp. 44–57, Jan. 2002.

[4] Martin A. Fischler and Robert C. Bolles, “Random sample consensus: a paradigm for model fitting with applications to image analysis and automated cartography,” *Commun. ACM*, vol. 24, no. 6, pp. 381–395, June 1981.